02

Comparison of *ab initio* and Lennard-Jones interaction potentials and their effect on particles beam scattering

© S.A. Nikitenko,[1] L.A. Varshavchik,[1] Z.G. Lyullin,[2] D.D. Galitsyn,[1] S.A. Starovoitov,[1] V.A. Bocharnikov,[1] E.E. Mukhin[1]

[1]Ioffe Institute,
194021 St. Petersburg, Russia
[2]St. Petersburg State Electrotechnical University „LETI"
197022 St. Petersburg, Russia
e-mail: lidia.varsh@mail.ioffe.ru

Received April 7, 2025
Revised May 12, 2025
Accepted May 13, 2025

The classical Lennard-Jones interaction potential was compared with *ab initio* potentials computed using the NWChem software. The *ab initio* calculations were performed using the MP2, CCSD and CCSD(T) methods with the following extrapolation to complete basis set limit. The resulting potentials were used to simulate the scattering of a boron atom beam in argon and helium gases using the KITe code. The elastic scattering angles, total and effective cross sections, as well as the scattering behavior of the atoms beam were compared for the different interatomic potentials. It was demonstrated that the Lennard-Jones potential, which is computationally much simpler than the accurate *ab initio* potential, exhibits deviations in the potential well and the repulsive regions. When scattering the model beam, atoms lose energy more rapidly with the Lennard-Jones potential than with the *ab initio* potential, although the shapes of the particle fronts are quite similar. The results of this work provide arguments for selecting an appropriate interatomic potential for elastic scattering modeling depending on the specific problem.

Keywords: NWChem, KITe, interatomic potential, *ab initio*, Lennard-Jones potential, elastic scattering, Monte-Carlo.

DOI: 10.61011/TP.2025.11.62228.55-25

Introduction

The numerical Monte Carlo simulation of the motion of atoms in a neutral gas is used in a number of tasks of modern physics, for example, when designing diagnostics of next-generation thermonuclear installations such as ITER, or when creating thin films by magnetron sputtering. To increase the accuracy of the simulation, it is important to have plausible data on the cross-sections of elastic scattering of particles. The classical approximation works well for describing particle collisions in the energy range of $0.01-100$ eV. At the same time, data on the interaction potential makes it possible to obtain all the necessary information about elastic scattering, scattering cross sections and angles, collision frequency and probability of collision with a background particle with certain components of the velocity vector. The accuracy of the collision data and, consequently, the nature of the particle motion in the background gas is determined by the accuracy of the interaction potential used.

At the moment, a large number of different model binary potentials of interatomic and intermolecular interaction have been developed, both purely repulsive and having a region of attraction. Of the latter, the Lennard-Jones potential [1–4] is widely known and most often used, combining simplicity and fairly high accuracy.

With the development of computer modeling, it has become possible to calculate particle interaction potentials using the it ab initio method, i.e. from the first fundamental principles without involving additional empirical assumptions or special models. For calculating potentials *ab initio* we used the NWChem [5] computational chemistry software package, which includes functions for quantum chemistry and molecular dynamics. NWChem is focused on scalability both in terms of the ability to efficiently solve complex tasks and in terms of using available parallel computing resources. NWChem is open source and freely available.

The purpose of this paper is to compare the classical Lennard-Jones interaction potential with the potential of *ab initio* calculated in NWChem. The interatomic potentials and all derived quantities in this work are calculated for three pairs of elements: boron atom with helium, neon and argon atoms. The decision on the choice of the type of interatomic potential is necessary to simulate a capacitive RF discharge in a noble gas, which is supposed to be used to clean the diagnostic optics of ITER from contamination by erosion products of the first boronized wall. Based on the interaction potentials, the parameters of elastic scattering were calculated and the results of modeling the scattering of a beam of boron atoms on a background gas performed in the code KITe [6,7] were compared.

1. Classical models for interaction potential

The principles of construction and an overview of the main two-particle interatomic interaction potentials used in molecular dynamic modeling of material properties are given in Ref. [8]. The simplest of them — the hard-sphere potential — is used for qualitative research of processes in dense liquids, amorphous and solids. Particles are considered as impenetrable, ideally hard spheres, and the potential is assumed to be zero if the distance between the atoms is less than the sum of the Van der Waals radii of the atoms, and equal to infinity in the opposite case. A slightly more realistic variation of this model is the potential of the Sutherland. Other two-particle models include the Lennard-Jones potentials [9], Morse potentials [10], and Buckingham potentials [11]. All of them are a continuous function of the distance between the atoms. The potential parameters are determined individually for each pair of atoms so that the analytical function best matches the experimental data.

The Lennard-Jones potential was originally intended to study the thermodynamic properties of noble gases. At short distances, atoms repel each other due to overlapping electron clouds, and at long distances there is a weak Van der Waals attraction. The potential has the form

$$U(r) = 4 \in \left[\left(\frac{\sigma}{r}\right)^{12} - \left(\frac{\sigma}{r}\right)^{6}\right],$$

where $\in$ is the depth of the potential well (characterizes the force of interaction), and σ is the distance at which the potential energy is zero (a parameter depending on the type of particles). For a pair of atoms, σ is equal to the sum of the Van der Waals radii of the atoms, and $\in$ is calculated as the geometric average of the values of the depth of the potential well of each atom. For heavy atoms, $\in$ can be assumed to be equal to the boiling point of this substance.

The Morse potential has been proposed to describe the vibrational energy levels of diatomic molecules and is widely used in molecular spectroscopy and studies of the crystalline properties of solids. Compared to the Lennard-Jones potential, Morse replaced the power dependence with the exponential one, as it better described experimentally observed energy levels. The long-range part agrees well with experimental data, but at zero the potential has a finite value, which is impossible, since atoms cannot be located at one point in space. Nevertheless, the Morse potential quite realistically describes the energy levels of diatomic molecules.

In this paper, we will use the Lennard-Jones potential for comparison with the *ab initio* potentials calculated in NWChem due to its mathematical simplicity and computational efficiency. This potential is described by only two parameters, which greatly simplifies model configuration and data processing. The versatility of the Lennard-Jones potential makes it possible to model both short-range repulsive and long-range attractive forces in various systems, including gases, liquids, and solids. In addition, the Lennard-Jones potential demonstrates good consistency with experimental data for many simple systems, which makes it a convenient tool for predicting thermodynamic and structural properties.

2. Quantum chemical methods for calculating potentials in NWChem

The methods of modern quantum chemistry of the *ab initio* group — from first principles — are based [12] on solving the Schrodinger equation by consistently applying simplifying approximations. Such methods include the Moeller-Plesset perturbation theory methods (MP2 [13–15], MP4 [16]), the Brueckner doubles method (BD) [17] and the Hartree-Fock method (HF), which includes coupled cluster methods (CC, their variants CCSD [18–20], CCSD(T) [21]) and configuration interaction methods (CI [22], CIS [23], CISD [24,25], MCSCF [26], CASSCF [27]). The Hartree-Fock method is fundamental because it allows you to form a wave function that is an initial approximation for other methods.

According to the Hartree-Fock method, the Schrodinger equation is solved by reducing a multiparticle problem to a single-particle one, assuming that each particle moves in an averaged self-consistent field created by all other particles of the system. The construction of a self-consistent field can be carried out either by the method of successive approximations (originally proposed by Hartree), or by the direct variational method [5]. The disadvantage of the method in its original form is the low accuracy of determining the energy of the system, due to the lack of consideration of the correlation interaction of electrons. In this regard, the method is currently used, as a rule, in combination with various additional methods that make it possible to determine the correlation energy of electrons (post-Hartree-Fock methods).

The coupled cluster method allows calculations to be performed with full iterative processing of single and double correlations and non-iterative inclusion of the effects of triple correlations using perturbation theory. A variation of the CCSD method solves nonlinear equations, taking into account correlation effects at the level of one- and two-electron excitations, which makes it significantly more accurate than methods at the level of perturbation theory, such as MP2. The CCSD(T) method is an extension of CCSD and includes correlation effects from three-electron excitations based on perturbation theory. This method is often referred to as the „gold standard“ [28–30] of quantum chemistry due to its high accuracy at an acceptable computational cost.

Among the Moeller-Plesset methods, the MP2 method is the most common - second-order perturbation theory for correlation energy. It is less accurate at short distances than CCSD(T) [29]. Using higher-order MP is impractical, because they require high computational costs.

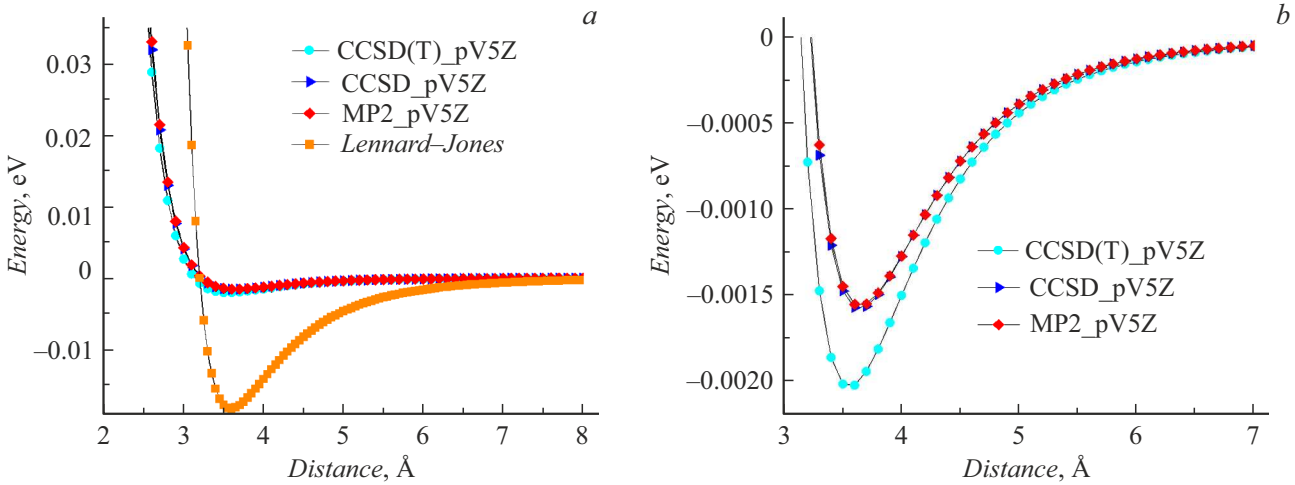

Figure 1. Interatomic interaction potentials for a pair of boron-helium atoms calculated in the NWChem program using CCSD, CCSD(T), and MP2 methods. The Lennard-Jones potential is also given. The graphs (*a*) and (*b*) are presented at different scales.

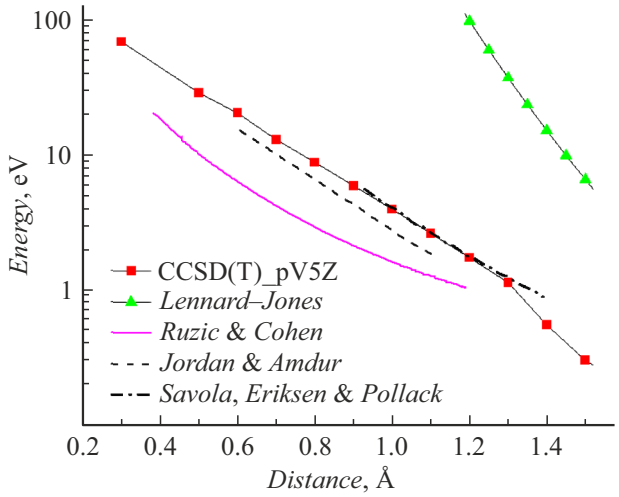

Figure 2. The Lennard-Jones potentials (green curve) and *ab initio* (red), calculated in NWChem using the CCSD(T) method with the pV5Z basis set, as well as experimental curves (pink and two dotted) for a pair of helium atoms.

A detailed description of the potential calculations *ab initio* in the NWChem program is given, for example, in Ref. [31]. A comparison of the types of the interatomic potential function for a system of boron and helium atoms calculated using the MP2, CCSD, CCSD(T), and Lennard-Jones methods is shown in Fig. 1. The Lennard-Jones potential function does not repeat the potentials *ab initio* either in the area of the potential well or in the repulsion zone (the positions of the potential well are close) and, since it has only two parameters, it is impossible to achieve a good shape match. Among the potentials *ab initio*, the CCSD and MP2 methods give almost an exact match, but the graphs differ from the more accurate CCSD(T) method by the lower depth of the potential well.

Let us compare (Fig. 2) the graphs of the Lennard-Jones and *ab initio* potentials with the experimental curves [32]. It can be seen that the potential curve *ab initio* is much closer to the experimental ones than the Lennard-Jones potential curve.

In addition to the modeling method, the accuracy of the calculated potential is influenced by the selected basis set of functions. In the calculation process, the desired wave function is represented as a linear combination of basis functions. This makes it possible to convert partial differential equations into algebraic equations suitable for efficient computer simulation.

Some of the most widely used basis sets, developed in Ref. [33], are designed to systematically converge post-Hartree-Fock computations to the limit of the complete basis set using empirical extrapolation methods [34]. Such sets include sequentially increasing shells of polarization (correlating) functions, and are denoted as cc-pVNZ, where N = D, T, Q, 5, 6, etc., etc. (where D = double, T = triple, etc.), „cc-p“ means „correlationally matched polarized“, and „*V*“ indicates that these are basis sets with valence only. Currently, such „correlation-consistent polarized“ basis sets are widely used and are the generally accepted standard for correlated or post-Hartree-Fock computations [33,35].

In addition, when modeling the interaction of pairs of atoms, including those located far from each other, for accurate calculations, it is necessary to add diffuse functions to describe long-range interactions, such as Van der Waals forces (aug-cc-pVnZ bases). A comparison of the types of the interatomic potential function for a pair of helium atoms calculated by the CCSD(T) method on various basis sets cc-pVDZ; cc-pVTZ; cc-pVQZ and cc-pV5Z is shown in Fig. 3. As the accuracy of the basis sets increases, the potential function decreases, the minimum position shifts to smaller distances, while the functions become closer and tend to a certain limit that will correspond to the full basis

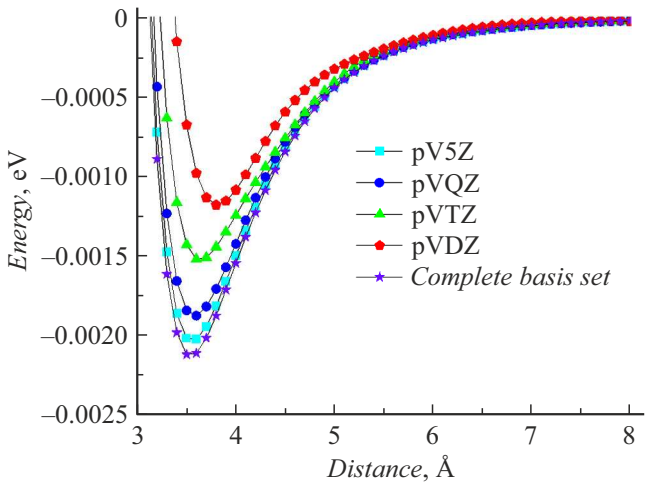

Figure 3. The interatomic interaction potentials calculated in the NWChem program for a pair of boron-helium atoms by the CCSD(T) method using bases of varying accuracy, as well as the extrapolated potential corresponding to the full basis set.

set. This limit can be obtained using the approximation formula [31,36,37]:

$$A(x) = A(\infty) + Be^{-(X-1)} + Ce^{-(X-1)^2},$$

where $X = 2,\ 3,\ 4,\ 5$ is the basis number, $A(x)$ is the value of the potential, and $A(\infty)$ is the desired approximate value. The potential function obtained as a result of solving this system of linear equations and corresponding to the complete basis set is also shown in Fig. 3.

3. Comparison of calculated elastic scattering parameters

Based on various functions of the interatomic interaction potentials (hard spheres, Lennard-Jones, and *ab initio*), the parameters of elastic scattering reactions were calculated for comparison: scattering angles depending on the target parameter, total and transport scattering cross sections depending on energy. The calculation algorithm is given in Ref. [6]. The motion of an incoming particle is modeled in the center of mass system. Fig. 4 shows the scattering trajectories of a boron atom on noble gas atoms for two types of Lennard-Jones potentials (Fig. 4, *a*) and *ab initio* (Fig. 4, *b*), calculated in the NWChem program using the CCSD(T) method using extrapolation to match the full basis set (no trajectories are constructed for the potential of hard spheres, since the scattering angle is calculated directly using the classical formula). The aiming parameters are the same for each pair of elements and are selected so as to show the trajectories of attraction (in green), repulsion (in blue) and capture of the particle into orbit (in red).

The scattering angle in the center of mass system is calculated as the angle of deviation of the velocity vector of the incident particle after the scattering act from the initial direction, i.e., the angle of trajectory change. Comparing the scattering trajectories at different potentials for each pair

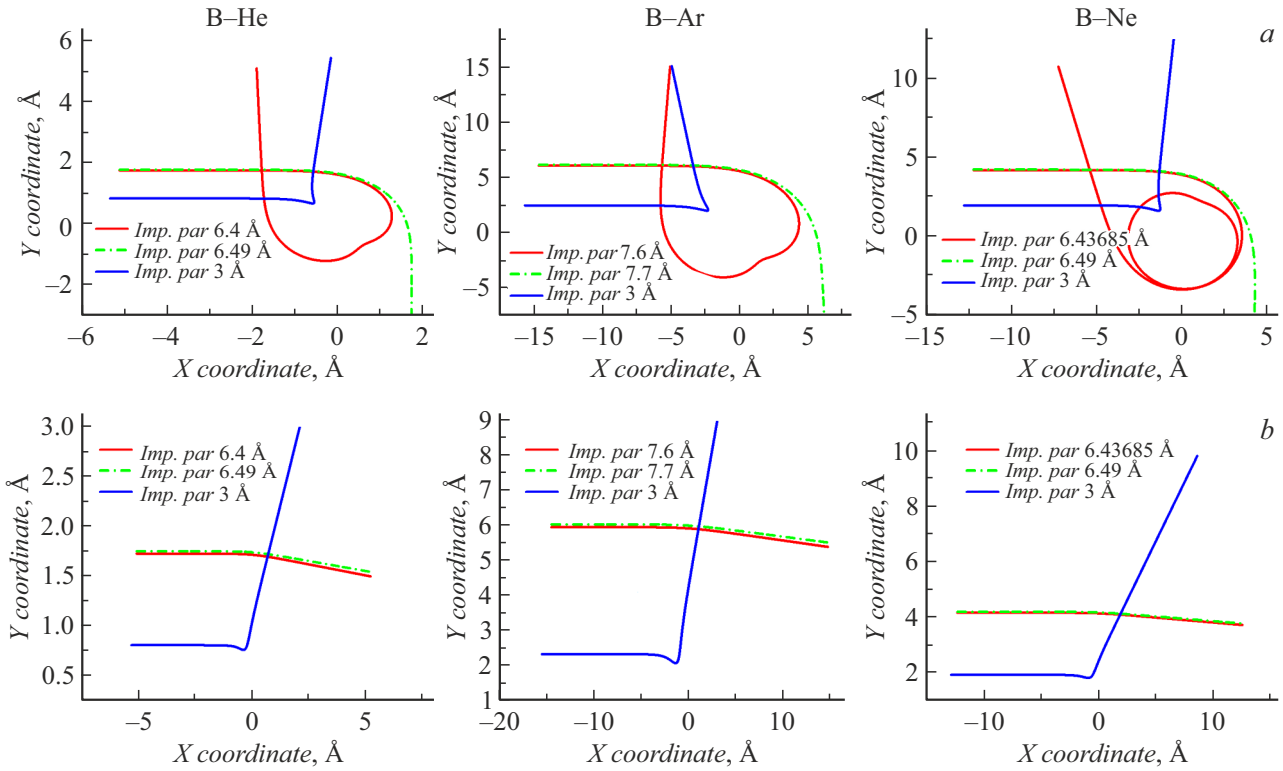

Figure 4. Scattering trajectories in the center of mass system; *a* — with the Lennard-Jones interaction potential, *b* — with interaction potentials obtained by extrapolation from the results of calculations in NWChem.

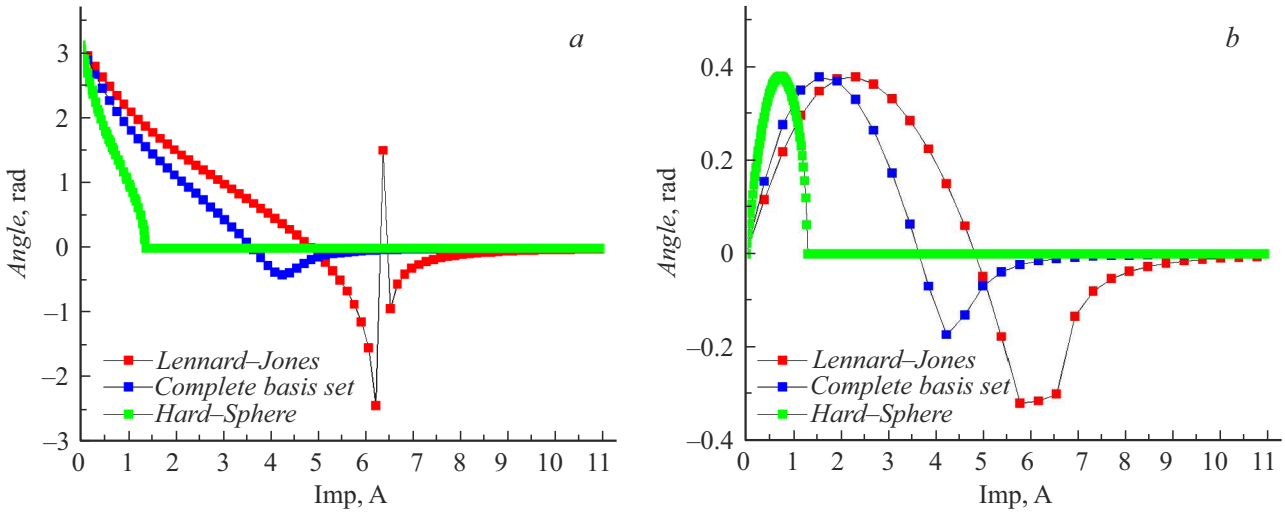

Figure 5. Dependence of scattering angles on the target parameter, calculated from the Lennard-Jones potentials of hard spheres and obtained by extrapolation *ab initio* in the NWChem program for pairs of elements B-Ne (*a*) and B-He (*b*).

of elements in Fig. 4, one can see a significant difference in the obtained scattering angles and the nature of their dependence on the aiming parameters. This difference will be further observed for all derived quantities, scattering cross-sections, collision frequency, etc. The scattering angle as a function of the target parameter for the potentials of hard spheres, Lennard-Jones, and it ab initio is shown in Fig. 5. For the scattering trajectory of a boron atom off a neon atom in the Lennard-Jones potential (blue curve), a distinct „kick-out" point with a positive angle is clearly visible at the distance corresponding to the potential well. It is for this point that the „capture" trajectory is plotted in Fig. 4, *a*, square B-Ne (red curve).

The scattering cross section in the center of mass system is calculated as the area of a circle $S = \pi b^2$ with radius b — with an aiming parameter at which the scattering angle is 1° (Fig. 6). Acts of scattering by less than 1° will not be taken into account.

The scattering transport cross section in the laboratory coordinate system (Fig. 7) is calculated using the formula (using the expression $d\sigma = 2\pi p dp$):

$$\sigma_T = \int_0^{\pi} \frac{d\sigma}{d\Omega}(1 - \cos\theta)d\Omega = \int_0^{\pi}(1 - \cos\theta(p))2\pi p dp.$$

Here p is the target parameter, θ is the scattering angle, σ is the scattering cross section. The integration limit is selected for each energy equal to the target parameter, which gives a scattering angle of 1°.

It can be seen that the total and transport cross sections, firstly, have a nonlinear dependence on energy, and secondly, they differ both in shape (the nonlinear dependence on energy manifests itself in different ways) and in absolute values (Table 1) when calculated using Lennard-Jones potentials and *ab initio*, obtained by extrapolating calculations in the NWChem program. Next, it will be

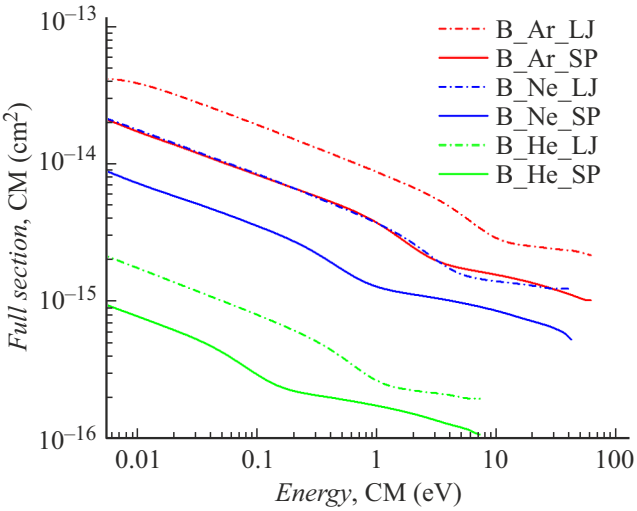

Figure 6. The total scattering cross sections as a function of energy in the center of mass system, calculated from the Lennard-Jones potentials and obtained by extrapolation *ab initio* (NWChem).

shown what differences in the nature of the motion of a beam of atoms in a neutral gas lead to the choice of the potential of interatomic interaction.

4. Scattering of a model beam of atoms at different potentials

Using the KITe code, we will simulate and compare the scattering pattern of a beam of boron atoms in helium using various interatomic potentials: hard spheres, Lennard-Jones potentials, and *ab initio* potentials calculated from the first principles in the NWChem program. The simulation takes into account the thermal motion of gas atoms. The

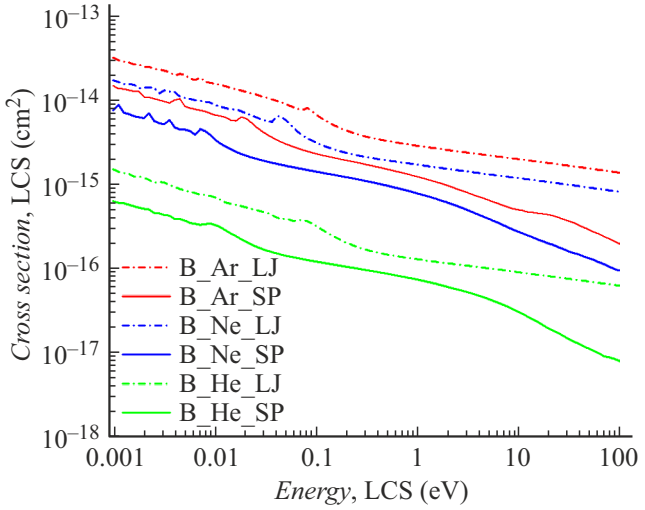

Figure 7. Transport cross sections of scattering as a function of energy in a laboratory system, calculated from Lennard-Jones potentials and obtained by extrapolation *ab initio*.

Table 1. The ratio of the total and transport cross-sections calculated according to the Lennard-Jones potential to the cross-sections calculated according to the potential *ab initio*

Section	B-He	B-Ar	B-Ne
Complete sections $\sigma_{LJ}/\sigma_{abinitio}$	2.08	2.14	2.24
Transport sections $\sigma^T_{LJ}/\sigma^T_{abinitio}$	2.87	3.04	3.34

temporal evolution of the beams is shown in Fig. 8. In all three cases, the beam of boron atoms starts from a surface 0.01 mm wide, which can be considered point-like relative to the characteristic distances at which the beam is scattered. The helium pressure is 1 Pa, the temperature is 300 K, the energy of the boron atoms at the beginning of the motion is 10 eV. The figures are given for time points 1.4, 3.6, 6.4, and 12 μs after the start of movement.

The beam propagation range (the position of the front) is determined by particles that have not collided and have an initial energy, and therefore is the same for all three cases. The key differences are visible in the shape of the beam and the tendency of energy loss by boron atoms. When using the potential of hard spheres, a narrow, arrow-like beam with a high directivity is formed. However, due to the mechanical nature of collisions, particles lose energy much faster than in other models (with the exception of a group of particles at the front of the beam that did not have time to undergo a collision, so the average beam energy is not so small). The average energy of boron beam atoms during scattering in helium at time 12 μs for various interatomic potentials is shown in Table 2. With the Lennard-Jones potential, the interatomic forces of attraction and repulsion are taken into account, so the beam becomes wider and has a spherical front, and the energy of the particles after scattering is preserved better than in the model of hard spheres. The shape of the beam using the potential *ab initio* (NWChem) turns out to be similar to the shape of the beam obtained using the Lennard-Jones model, but the potential *ab initio* provides the best energy conservation during scattering.

Let us give the time evolution of the scattering of beams of boron atoms in argon (Fig. 9). The conditions (temperature, gas pressure, and the energy of boron atoms at the beginning of motion) are set to be the same as during scattering in helium. The figures are given for time points 1.4, 6.4, and 12 μs after the start of motion (i.e., compared with scattering in helium, there is no second time point equal to 3.6 μs). Unlike helium (atomic mass 4.003 Da), argon (39.948 Da) is significantly heavier than boron (10.811 Da), which is why boron atoms appear during scattering, reflecting off argon and changing the direction of motion to the opposite.

The patterns in the scattering of a boron beam in argon with different interatomic potentials remain the same as in the case of boron scattering in helium: in the potential of hard spheres, the beam has an arrow-like shape, whereas in the Lennard-Jones and ab-initio potentials, the beam has a spherical front. In the Lennard-Jones potential, particles lose energy (Table 2) and directional motion faster than in the potential *ab initio*.

Conclusion

Using the NWChem computational chemistry software package using the MP2, CCSD, and CCSD(T) methods, the interatomic interaction potentials for boron atoms with helium, neon, and argon atoms were calculated. For the potentials obtained by the CCSD(T) method using bases of varying accuracy, the potential corresponding to the complete basis set was constructed using extrapolation. The scattering trajectories of a boron atom on helium/neon/argon at various impact parameters were simulated in the KITe code for this potential, as well as for comparison of the hard-sphere potential and the Lennard-Jones potential. The scattering angles, total scattering cross sections, and transport cross sections were calculated. The scattering of a monoenergetic beam of boron atoms by atoms of the background gas helium and argon was simulated, taking into account the thermal motion of the gas. It is shown that in both gases (helium and argon), when using the potential of hard spheres, the beam of boron atoms has a directional arrow-like shape during scattering, while at the Lennard-Jones and *ab initio* potentials, the particles scatter in a cloud with a radial front. When using the potential *ab initio*, the directional motion of particles (the shape of the front) persists longer, and the loss of energy by particles occurs much more slowly than with the Lennard-Jones potential. Of course, using the potential *ab initio* in modeling particle transport will allow for more accurate results, however, in the absence of such an opportunity, using the classical Lennard-Jones potential will show a fairly

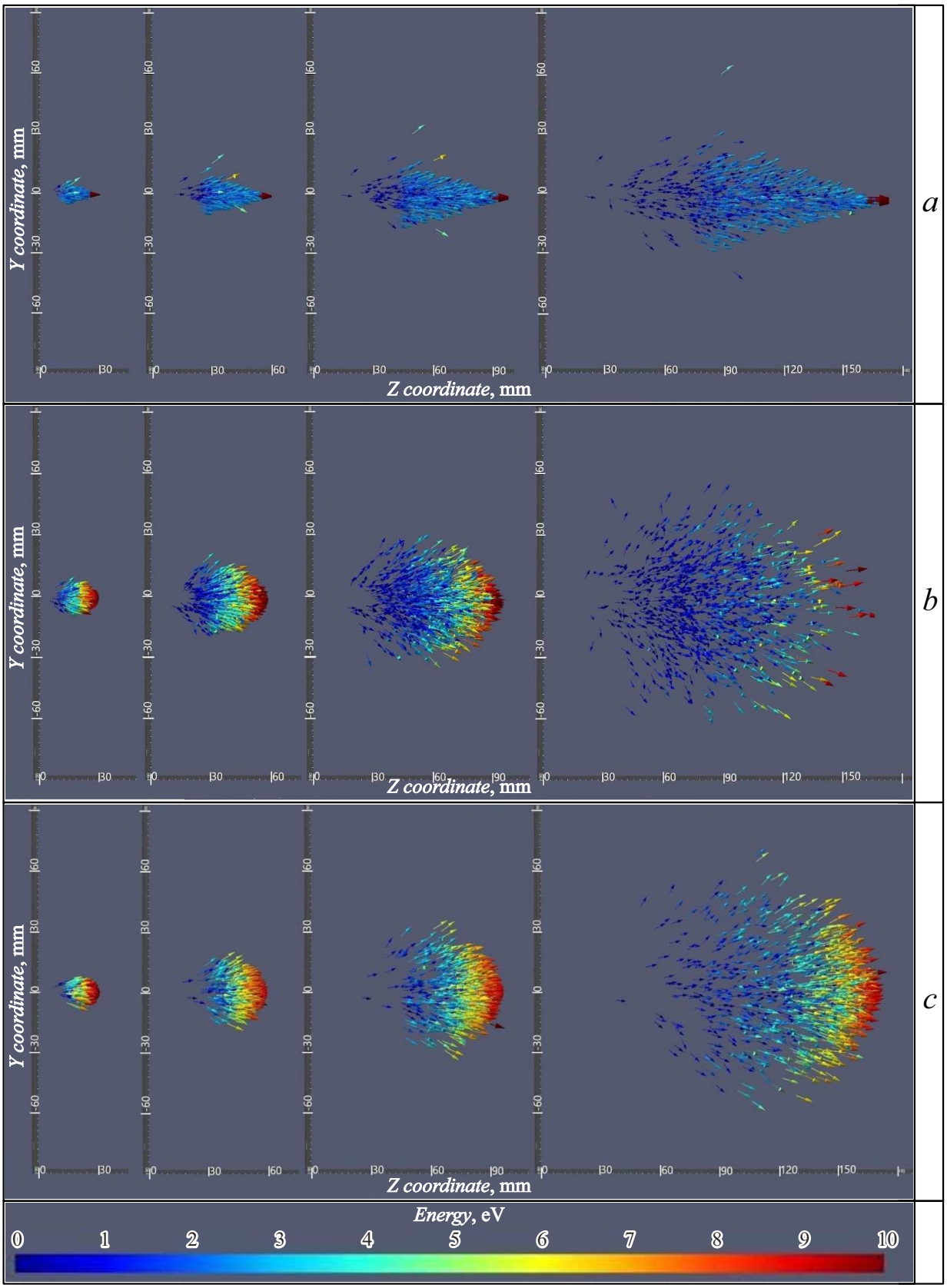

Figure 8. Scattering of a beam of boron atoms with energies of 10 eV in helium with a pressure of 1 Pa and a temperature of 300 K at time points 1.4, 3.6, 6.4 and 12 μs after the start of motion. Interatomic potentials were used: *a* — hard spheres, *b* —Lennard-Jones, *c* —*ab initio* (calculated in NWChem).

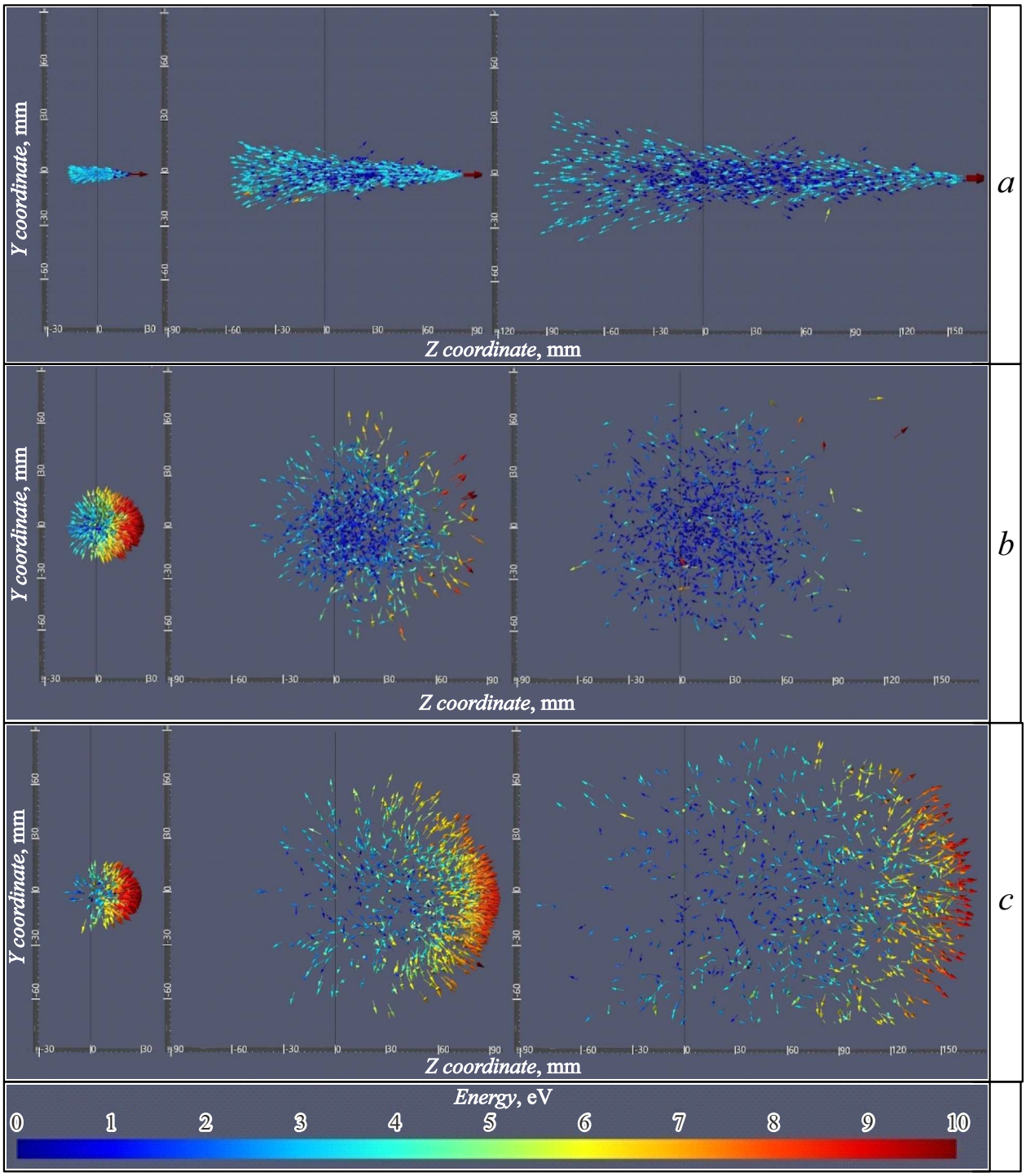

Figure 9. Scattering of a beam of boron atoms with energies of 10 eV in argon with a pressure of 1 Pa and a temperature of 300 K at time points 1.4, 6.4 and 12 μs after the start of motion. Interatomic potentials were used: *a* — hard spheres, *b* —Lennard-Jones, *c* —*ab initio* (calculated in NWChem).

Table 2. Average energy (eV) of boron atoms during scattering in helium and argon at time 12 μs

Atoms	Potential of hard spheres	Potential of Lennard-Jones	Potential *ab initio* (NWChem)
He	3.89	1.43	4.52
Ar	2.42	1.01	4.72

reliable scattering pattern, taking into account corrections for excessive loss of particle energy when analyzing the results.

Acknowledgments

The authors would like to thank one of the developers of the NWChem software package — Edoardo Aprà — for clarifications and assistance when working with the program.

Conflict of interest

The authors declare no conflict of interest.

References

[1] N. Ohtori, Y. Ishii. Phys. Rev. E, **91**, 012111 (2015).
[2] B. Vorselaars. J. Chem. Phys., **142**, 114115 (2015).
[3] L. Wang, N. Xu. Phys. Rev. Lett., **112**, 055701 (2014).
[4] N. Sharifi-Mood, J. Koplik, C. Maldarelli. Phys. Rev. Lett., **111**, 184501 (2013).
[5] E. Aprà, E.J. Bylaska, W.A. de Jong, N. Govind, K. Kowalski, T.P. Straatsma, M. Valiev, H.J.J. van Dam, Y. Alexeev, J. Anchell, V. Anisimov, F.W. Aquino, R. Atta-Fynn, J. Autschbach, N.P. Bauman, J.C. Becca, D.E. Bernholdt, K. Bhaskaran-Nair, S. Bogatko, P. Borowski, J. Boschen, J. Brabec, A. Bruner, E. Cauët, Y. Chen, G.N. Chuev, C.J. Cramer, J. Daily, M.J.O. Deegan, T.H. Dunning Jr, M. Dupuis, K.G. Dyall, G.I. Fann, S.A. Fischer, A. Fonari, H. Früchtl, L. Gagliardi, J. Garza, N. Gawande, S. Ghosh, K. Glaesemann, A.W. Götz, J. Hammond, V. Helms, E.D. Hermes, K. Hirao, S. Hirata, M. Jacquelin, L. Jensen, B.G. Johnson, H. Jónsson, R.A. Kendall, M. Klemm, R. Kobayashi, V. Konkov, S. Krishnamoorthy, M. Krishnan, Z. Lin, R.D. Lins, R.J. Littlefield, A.J. Logsdail, K. Lopata, W. Ma, A.V. Marenich, J. Martin del Campo, D. Mejia-Rodriguez, J.E. Moore, J.M. Mullin, T. Nakajima, D.R. Nascimento, J.A. Nichols, P.J. Nichols, J. Nieplocha, A. Otero-de-la-Roza, B. Palmer, A. Panyala, T. Pirojsirikul, B. Peng, R. Peverati, J. Pittner, L. Pollack, R.M. Richard, P. Sadayappan, G.C. Schatz, W.A. Shelton, D.W. Silverstein, D.M.A. Smith, T.A. Soares, D. Song, M. Swart, H.L. Taylor, G.S. Thomas, V. Tipparaju, D.G. Truhlar, K. Tsemekhman, T. Van Voorhis, Á. Vázquez-Mayagoitia, P. Verma, O. Villa, A. Vishnu, K.D. Vogiatzis, D. Wang, J.H. Weare, M.J. Williamson, T.L. Windus, K. Woliński, A.T. Wong, Q. Wu, C. Yang, Q. Yu, M. Zacharias, Z. Zhang, Y. Zhao, R.J. Harrison. J. Chem. Phys., **152** (18), 184102 (2020).
[6] L.A. Varshavchik, N.A. Babinov, P.A. Zatylkin, A.A. Chironova, Z.G. Lyullin, Al.P. Chernakov, A.M. Dmitriev, I.M. Bukreev, E.E. Mukhin, A.G. Razdobarin, D.S. Samsonov, V.A. Senitchenkov, S.Yu. Tolstyakov, I.T. Serenkov, V.I. Sakharov. Plasma Phys. Controlled Fusion, **63** (2), 025005 (2021).
[7] L.A. Varshavchik, D.D. Galitsyn, E.A. Starovoitov, V.A. Bocharnikov, S.A. Nikitenko, E.E. Mukhin. Pis'ma v ZhTF, **51** (3), 26 (2025) (in Russian).
DOI: 10.61011/PJTF.2025.03.59816.20011
[8] A.A. Selezenev. *Osnovy metoda molekulyarnoj dinamiki: uchebno-metodicheskoe posobie* (SarFTI, Sarov, 2017) (in Russian).
[9] J.E. Lennard-Jones. Proc. Roy. Soc., **A106**, 463 (1924).
[10] P.M. Morse. Phys. Rev., **34**, 57 (1929).
[11] R.A. Buckingham. Proc. Roy. Soc., **A168**, 264 (1938).
[12] S.K. Ignatov. *Kvantovo-himicheskoe modelirovanie atomno-molekulyarnyh processov: uchebnoe posobie* (NNGU im. N.I.Lobachevskogo, Nizhnij Novgorod, 2019) (in Russian).
[13] M. Head-Gordon, J.A. Pople, M.J. Frisch. Chem. Phys. Lett., **153**, 503 (1988).
[14] S. Saebø, J. Almlöf. Chem. Phys. Lett., **154**, 83 (1989).
[15] M.J. Frisch, M. Head-Gordon, J.A. Pople. Chem. Phys. Lett., **166**, 275 (1990).
[16] K. Raghavachari, J.A. Pople. Int. J. Quantum Chem., **14**, 91 (1978).
[17] N.C. Handy, R.D. Amos. Chem. Phys. Lett., **98**, 428 (1983).
[18] G.D. Purvis, R.J. Bartlett. J. Chem. Phys., **76**, 1910 (1982).
[19] G.E. Scuseria, C.L. Janssen, H.F. Schaefer III. J. Chem. Phys., **89**, 7382 (1988).
[20] G.E. Scuseria, H.F. Schaefer. J. Chem. Phys., **90**, 3700 (1989).
[21] J.A. Pople, M. Head-Gordon, K. Raghavachari. J. Chem. Phys., **87**, 5968 (1987).
[22] C.D. Sherrill, H.F. Schaefer III. Advances in Quantum Chemistry, **34**, 143 (1999).
[23] J.B. Foresman, M. Head-Gordon, J.A. Pople, M.J. Frisch. J. Phys. Chem., **96**, 135 (1992).
[24] M. Head-Gordon, R.J. Rico, M. Oumi, T.J. Lee. Chem. Phys. Lett., **219**, 21 (1994).
[25] M. Head-Gordon, D. Maurice, M. Oumi. Chem. Phys. Lett., **246**, 114 (1995).
[26] A.C. West, J.D. Lynch, B. Sellner, H. Lischka, W.L. Hase, T.L. Windus. Theor. Chem. Acc., **131**, 1123 (2012).
[27] J.B. Foresman, A.E. Frisch. *Exploring chemistry with electronic structure methods: A guide to using Gaussian*, 2nd edition (PA: Gaussian Inc., Pittsburgh, 1996)
[28] Electronic source. Available at:
https://habr.com/ru/articles/580770/
[29] Electronic source. Available at:
https://www.youtube.com/watch?v=oU1zO2bPPB4&list=PLm8ZSArAXicL3jKr_0nHHs5TwfhdkMFhh&index=100
[30] R. Hellmann, E. Bich, E. Vogel. Molecular Phys., **105** (23–24), 3013 (2007).
DOI: 10.1080/00268970701730096
[31] D.S. Bezrukov, N.N. Kleshchina, I.S. Kalinina, A.A. Buchachenko. J. Chem. Phys., **150**, 064314 (2019).
DOI: 10.1063/1.5071457
[32] D.N. Ruzic, S.A. Cohen. J. Chem. Phys., **83**, 5527 (1985).
DOI: 10.1063/1.449674
[33] T.H. Dunning Jr. J. Chem. Phys., **90** (2), 1007 (1989).
[34] A.P. Rendell, T.J. Lee, A. Komornicki, S. Wilson. Theoreticachimica Acta, **84** (4), 271 (1993).
[35] S. Lehtola. Intern. J. Quant. Chem., **119** (19), e25968 (2019).
[36] K.A. Peterson, D.E. Woon, T.H. Dunning Jr. J. Chem. Phys., **100**, 7410 (1994). DOI: 10.1063/1.46688433
[37] D. Feller, J.A. Sordo. J. Chem. Phys., **112**, 5604 (2000).
DOI: 10.1063/1.481135

Translated by A.Akhtyamov